

This article may be downloaded for personal use only. Any other use requires prior permission of the author and AIP Publishing.

The following article appeared in *Journal of Applied Physics* 113, 17A912 (2013); and may be found at <https://doi.org/10.1063/1.4794988>

## Magnetic entropy change and refrigerant capacity of rapidly solidified TbNi<sub>2</sub> alloy ribbons

J. L. Sánchez Llamazares, C. F. Sánchez-Valdes, P. J. Ibarra-Gaytan, Pablo Álvarez-Alonso, P. Gorria, and J. A. Blanco

Citation: *Journal of Applied Physics* **113**, 17A912 (2013);

View online: <https://doi.org/10.1063/1.4794988>

View Table of Contents: <http://aip.scitation.org/toc/jap/113/17>

Published by the *American Institute of Physics*

---

### Articles you may be interested in

[Texture-induced enhancement of the magnetocaloric response in melt-spun DyNi<sub>2</sub> ribbons](#)

*Applied Physics Letters* **103**, 152401 (2013); 10.1063/1.4824073

[Enhanced refrigerant capacity in two-phase nanocrystalline/amorphous NdPrFe<sub>17</sub> melt-spun ribbons](#)

*Applied Physics Letters* **104**, 212401 (2014); 10.1063/1.4879544

[Table-like magnetocaloric effect in the Gd-Co-Al alloys with multi-phase structure](#)

*Applied Physics Letters* **104**, 072401 (2014); 10.1063/1.4865554

[Two successive magnetic transitions induced large refrigerant capacity in HoPdIn compound](#)

*Applied Physics Letters* **103**, 222405 (2013); 10.1063/1.4834815

[Field dependence of the magnetocaloric effect in materials with a second order phase transition: A master curve for the magnetic entropy change](#)

*Applied Physics Letters* **89**, 222512 (2006); 10.1063/1.2399361

[Effect of partial substitution of Ni by Co on the magnetic and magnetocaloric properties of Ni<sub>50</sub>Mn<sub>35</sub>In<sub>15</sub> Heusler alloy](#)

*Journal of Applied Physics* **109**, 07A916 (2011); 10.1063/1.3540696

---

**Scilight**

Sharp, quick summaries **illuminating**  
the latest physics research

Sign up for **FREE!**



## Magnetic entropy change and refrigerant capacity of rapidly solidified TbNi<sub>2</sub> alloy ribbons

J. L. Sánchez Llamazares,<sup>1,a)</sup> C. F. Sánchez-Valdes,<sup>2</sup> P. J. Ibarra-Gaytan,<sup>1</sup> Pablo Álvarez-Alonso,<sup>3</sup> P. Gorria,<sup>4</sup> and J. A. Blanco<sup>4</sup>

<sup>1</sup>Instituto Potosino de Investigación Científica y Tecnológica, Camino a la Presa San José 2055 Col. Lomas 4a, San Luis Potosí, S.L.P. 78216, Mexico

<sup>2</sup>Institut de Ciència de Materials de Barcelona, CSIC, Campus UAB, 08193 Bellaterra, Spain

<sup>3</sup>Departamento de Electricidad y Electrónica, Universidad del País Vasco (UPV/EHU), 48940 Leioa, Spain

<sup>4</sup>Departamento de Física, Universidad de Oviedo, Calvo Sotelo s/n, 33007 Oviedo, Spain

(Presented 15 January 2013; received 5 November 2012; accepted 3 December 2012; published online 13 March 2013)

The magnetocaloric effect in TbNi<sub>2</sub> alloy ribbons synthesized by rapid solidification was investigated. This material crystallizes in a superstructure of the cubic Laves phase structure type C15 (space group F-43m). The saturation magnetization and Curie temperature are  $M_S = 134 \pm 2 \text{ A m}^2 \text{ kg}^{-1}$  and  $T_C = 37 \pm 1 \text{ K}$ , respectively. For a magnetic field change of 5 T, the material shows a maximum magnetic entropy change  $|\Delta S_M^{\text{peak}}| = 13.9 \text{ J kg}^{-1} \text{ K}^{-1}$ , with a full-width at half-maximum  $\delta T_{\text{FWHM}} = 32 \text{ K}$ , and a refrigerant capacity  $RC = 441 \text{ J kg}^{-1}$ . The RC value is similar to those reported for other magnetic refrigerants operating within the temperature range of 10–80 K. Finally, it is worth noting that the use of rapid solidification circumvents the necessity for long-term high-temperature homogenization processes normally needed with these RNi<sub>2</sub> alloys. © 2013 American Institute of Physics. [<http://dx.doi.org/10.1063/1.4794988>]

Over the last two decades, the magnetocaloric (MC) properties of Laves phases have been extensively investigated. As a result, some compounds in the RCo<sub>2</sub>, RAl<sub>2</sub>, and RNi<sub>2</sub> systems (R = rare earth) have been referred to as promising magnetic refrigerants in the 10–80 K temperature range.<sup>1,2</sup> In particular, RNi<sub>2</sub> with R = Tb, Dy, or Er and related compounds have been proposed as suitable components to design a low-temperature magnetocaloric composite with a *table-like* temperature dependence of the magnetic entropy change  $\Delta S_M(T)$ .<sup>2–4</sup> Such a *table-like* shape of  $\Delta S_M(T)$  is a desirable feature for an ideal Ericsson-like refrigeration cycle,<sup>5</sup> and it is currently a topic of increasing interest in research with MC composites.<sup>6,7</sup> Recently, a theoretical model including both crystal-field and exchange interactions that considers the effect of magnetic fluctuations through the random phase approximation was developed to describe satisfactorily the experimental  $\Delta S_M(T)$  in RNi<sub>2</sub> compounds.<sup>8</sup> These calculations predict a large magnetic entropy change under a magnetic field change  $\mu_0 \Delta H$  of 5 T,  $\Delta S_M^{\text{peak}} \sim -27.9 \text{ J kg}^{-1} \text{ K}^{-1}$  for TbNi<sub>2</sub> along the [111] direction, while the values along [110] and [001] directions are  $-21.7 \text{ J kg}^{-1} \text{ K}^{-1}$  and  $-14.5 \text{ J kg}^{-1} \text{ K}^{-1}$ , respectively.<sup>8</sup> Owing to the anisotropic MC response of this material, the mean value of  $\Delta S_M^{\text{peak}}$  expected for a polycrystalline sample should be around  $-5.7 \text{ J mol}^{-1} \text{ K}^{-1}$  ( $-20.5 \text{ J kg}^{-1} \text{ K}^{-1}$ ). However, the measured value [ $\Delta S_M^{\text{peak}} \sim -4.0 \text{ J mol}^{-1} \text{ K}^{-1}$  ( $-14.5 \text{ J kg}^{-1} \text{ K}^{-1}$ )] in a bulk polycrystalline alloy is lower than the predicted value.<sup>9,10</sup> Moreover, the refrigerant capacity  $RC$ , which is an important figure of merit that allows the evaluation and comparison of magnetic coolants for refrigeration purposes,<sup>11,12</sup> can reach values over  $400 \text{ J kg}^{-1}$  for  $\mu_0 \Delta H = 5 \text{ T}$  in these alloys as we have shown below.

Until now, the TbNi<sub>2</sub> compound has been prepared using conventional melting techniques followed by long-term thermal annealing of more than 1 week at temperatures above 900 K.<sup>9,10,13,14</sup> It crystallizes in a cubic structure which is a superstructure (space group F-43m) of the C15 cubic Laves phase with a doubled *a*-axis with respect to the well-known Laves phase.<sup>15,16</sup> The Tb atoms are located at five nonequivalent crystallographic sites, but regularly ordered vacancies of the rare earth atoms were found at one of these five sites, namely the 4a sites (in Wyckoff notation); while the corresponding Ni atoms occupy four inequivalent sites. In this compound, only the Tb<sup>+3</sup> ions possess a magnetic moment,<sup>17,18</sup> being a ferromagnet with a Curie temperature,  $T_C = 36 \text{ K}$ , and with the easy magnetization axis along the [111] direction above 14 K.<sup>9,13</sup>

The present investigation was undertaken to produce rapidly solidified ribbons of the binary TbNi<sub>2</sub> intermetallic compound by using the melt-spinning technique as well as to determine their phase constitution and MC response. Herein, we show that the samples produced using a one-step rapid solidification process, which avoids the long-term high temperature heat treatment, exhibit MC properties that are similar to those previously reported for homogenized bulk samples. This technique has been successfully applied to produce different crystalline alloys of current interest as magnetocaloric materials such as LaFe<sub>13-x</sub>Si<sub>x</sub>,<sup>19</sup> (MnFe)<sub>2</sub>(PGe),<sup>20</sup> Gd<sub>5</sub>(SiGeSn)<sub>4</sub>,<sup>21</sup> and Ni-Mn-X Heusler alloys (X = Sn, In, Ga).<sup>22–24</sup> In all the cases, a single phase can be developed in the as-solidified alloy ribbons, or after a much shortened thermal annealing compared to their bulk counterpart.

Bulk alloys of nominal composition TbNi<sub>2</sub> were produced by arc melting from pure elements (Tb 99.9%, relative to the rare-earth content, and Ni 99.99%) under a controlled Ar atmosphere. Polycrystalline alloy ribbons were fabricated

<sup>a)</sup>Author to whom correspondence should be addressed. Electronic mail: jose.sanchez@ipicyt.edu.mx.

using a homemade melt spinning setup operating in an Ar environment at a wheel (copper) speed of  $20 \text{ ms}^{-1}$ .

X-ray diffraction (XRD) patterns of finely powdered samples were collected with a Bruker AXS model D8 Advance x-ray powder diffractometer using  $\text{Cu-K}\alpha$  radiation. Microstructure and elemental composition were determined with a FEI/Philips XL30 FEG ESEM. Analysis of the diffraction data, based on the Rietveld method, was carried out with the FULLPROF suite package.<sup>25</sup> Magnetic measurements were performed by vibrating sample magnetometry in a Quantum Design PPMS<sup>®</sup> EverCool<sup>®</sup> –9 T platform, in which the magnetic field  $\mu_0 H$  was applied along the ribbon axis to minimize the effect of the demagnetizing field. A set of isothermal magnetization curves,  $M(\mu_0 H)$ , were measured in the temperature range of 4–70 K with a maximum applied magnetic field of 5 T. The value of  $\Delta S_M$  at each temperature  $T$ , due to a change of the applied magnetic field from 0 to  $\mu_0 H_{\text{max}}$ , was calculated using the Maxwell relation.<sup>1,5</sup> In order to estimate the  $RC$  values from the  $\Delta S_M(T)$  curves, three different methods are used: (a) by finding the product  $|\Delta S_M^{\text{peak}}| \times \delta T_{\text{FWHM}}$  (hereafter referred to as  $RC-1$ ),<sup>5</sup> where  $\delta T_{\text{FWHM}} = T_{\text{hot}} - T_{\text{cold}}$  is the temperature range that corresponds to the full width at half maximum of the  $\Delta S_M(T)$  curve (here,  $\delta T_{\text{FWHM}}$  coincides with the temperature span of the thermodynamic cycle); (b) by calculating the integral, under the  $\Delta S_M(T)$  curves between  $T_{\text{hot}}$  and  $T_{\text{cold}}$  (hereafter referred to as  $RC-2$ );<sup>11</sup> and (c) by maximizing the product  $\Delta S_M \times \delta T$  below the  $\Delta S_M(T)$  curve (referred to as  $RC-3$ ).<sup>12,26</sup>

EDS analyses performed on the cross section and both ribbon surfaces of different ribbon flakes indicate that the chemical composition agrees (with an uncertainty of,  $\sim 0.1 \text{ wt. } \%$ ) with that of the starting bulk alloy ( $\approx 0.98:2$ , Tb:Ni). The room temperature XRD pattern is depicted in Figure 1(a). All of the observed diffraction peaks can be indexed as the Bragg reflections corresponding to the  $\text{TbNi}_2$  phase, with a superstructure C15 (space group  $F-43m$ , #216, *International Tables of X-ray Crystallography*) of the cubic Laves phase, and a refined lattice parameter  $a = 14.34 \pm 0.03 \text{ \AA}$ . The inset of Figure 1(a) shows a typical SEM micrograph of the ribbons fracture morphology. The ribbons exhibit micronic columnar grains with a tendency to grow along the entire ribbon thickness, with the longer axis perpendicular to the ribbon plane. The ribbon thickness varies between  $10 \mu\text{m}$  and  $12 \mu\text{m}$ .

Figure 1(b) shows the temperature dependence of the magnetization,  $M(T)$ , measured under an applied magnetic field of 5 mT (red closed circles) and 5 T (black open circles). The Curie temperature,  $T_C = 37 \pm 1 \text{ K}$ , was estimated from the low-field  $M(T)$  curve as the minimum of the  $dM/dT$  versus  $T$  variation (see inset), and coincides with the value reported for bulk alloys.<sup>9,13</sup> In addition, the  $dM/dT$  versus  $T$  curve also reveals a slight minimum ( $T_R \approx 15.5 \pm 1.0 \text{ K}$ ), which could be ascribed to the spin reorientation transition reported for bulk alloys at around 14 K, and confirmed by neutron diffraction, AC-magnetic susceptibility, and heat capacity measurements.<sup>13</sup> The negative slope in the low-field region of the Arrott's plots [shown in the right inset of Figure 2(a)] below 16 K also indicates such a first-order magnetic phase transition, while the positive slope around  $T_C$  confirms the second-order character of the main ferro-to-paramagnetic

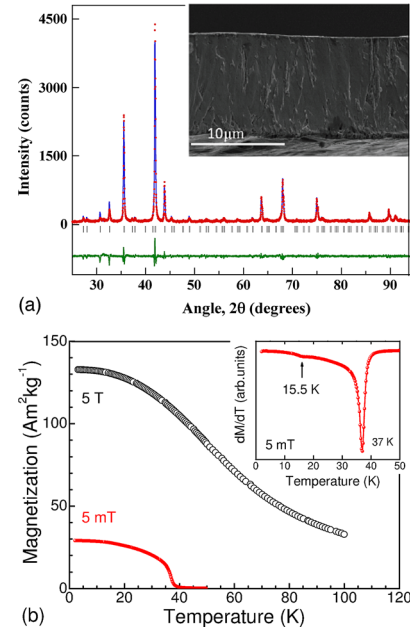


FIG. 1. (a) The room temperature x-ray powder diffraction pattern of  $\text{TbNi}_2$ . Inset: typical cross-sectional microstructure of  $\text{TbNi}_2$  ribbons. (b)  $M(T)$  curves measured in the field-cooled regime at 5 mT (full red symbols) and 5 T (open symbols). Inset: the  $dM/dT$  versus  $T$  curve at 5 mT.

transition. From a fit to an approach-to-saturation law, we have determined the saturation magnetization  $M_s = 134 \pm 2 \text{ A m}^2 \text{ kg}^{-1}$  at  $T = 2 \text{ K}$ , in good agreement with the value reported for bulk alloys.<sup>13</sup> Thus, the ribbons show intrinsic magnetic properties that are similar to those of the bulk polycrystalline alloys despite being formed by a non-equilibrium technique.

Figure 2(a) shows the  $\Delta S_M(T)$  curves for the field changes of 2 and 5 T. For  $\mu_0 \Delta H = 5 \text{ T}$  (2 T), the ribbon exhibits a large value for the maximum magnetic entropy change  $|\Delta S_M^{\text{peak}}| = 13.9$  (8.0)  $\text{J kg}^{-1} \text{ K}^{-1}$  at 37 K, as well as a full width at half maximum for the  $|\Delta S_M(T)|$  curve of  $\delta T_{\text{FMHW}} = 32$  (20) K, in the temperature interval of  $24 \text{ K} \leq T \leq 56 \text{ K}$  ( $27 \text{ K} \leq T \leq 47 \text{ K}$ ). The first-order spin reorientation transition gives rise to a small shoulder in the  $|\Delta S_M(T)|$  curve at around 15 K, which is more pronounced for  $\mu_0 \Delta H = 2 \text{ T}$ , in agreement with previous reports.<sup>9,13</sup> In Table I, the magnetocaloric properties are summarized for these as-quenched ribbons. Interestingly, the experimental value of  $|\Delta S_M^{\text{peak}}| = 13.9 \text{ J kg}^{-1} \text{ K}^{-1}$  obtained for a magnetic field change  $\mu_0 \Delta H$  of 5 T for the  $\text{TbNi}_2$  ribbon is around 4%, lower than the measured value ( $14.5 \text{ J kg}^{-1} \text{ K}^{-1}$ ) found for bulk polycrystalline alloys of this material.<sup>9,10</sup> Furthermore, it is less than almost one-third of that predicted by the mean field approximation including the effect of magnetic fluctuations through the random phase approximation, for a polycrystalline sample,  $|\Delta S_M^{\text{peak}}| \sim 20.5 \text{ J kg}^{-1} \text{ K}^{-1}$  [see Ref. 8 for the calculated values]. The experimental values for the ribbons and the polycrystalline bulk  $\text{TbNi}_2$  samples are consistent and may be understood if it is assumed that in the ribbons all the orientations of the easy-axis [111] magnetization with respect to the applied magnetic field are possible, suggesting that the azimuthal average will give a similar mean value for the ribbons and bulk polycrystalline samples. This assumption is supported by the x-ray diffraction pattern in which all of the Bragg reflection peaks for this crystal

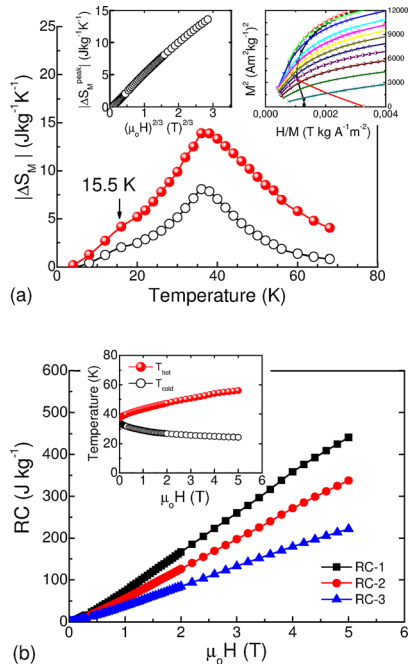


FIG. 2. (a)  $\Delta S_M(T)$  curve(s) at  $\mu_0\Delta H = 2$  and 5 T. Left inset:  $|\Delta S_M^{\text{peak}}|$  as a function of  $(\mu_0 H)^{2/3}$ . Right inset: Low-field region of the Arrott plots in the temperature range between 2 and 36 K. (b) Field dependence of  $RC-1$ ,  $RC-2$ , and  $RC-3$ . Inset: The field dependence of the temperatures  $T_{\text{hot}}$  and  $T_{\text{cold}}$  (i.e.,  $\delta T_{\text{FWHM}} = T_{\text{hot}} - T_{\text{cold}}$ ).

structure are observed, an indication that all orientations of the crystallites are present, as occurs in conventionally formed polycrystalline samples. The difference between the predicted value from theory quoted above and the experimental values requires further investigation to ascertain the reason for this discrepancy. Nonetheless, the dependence of  $|\Delta S_M^{\text{peak}}|$  on  $(\mu_0 H)^{2/3}$  [see left inset in Figure 2(a)] is consistent with the description given in Ref. 5 for materials with second-order transitions.

Figure 2(b) displays the field dependence of the refrigerant capacity  $RC-1$ ,  $RC-2$ , and  $RC-3$  and the characteristic temperatures,  $T_{\text{hot}}$  and  $T_{\text{cold}}$  (inset). Although the refrigerant capacity of the bulk  $\text{TbNi}_2$  alloys has not been reported, for a field change of 5 T  $RC-1$  values of  $423 \text{ J kg}^{-1}$  ( $|\Delta S_M^{\text{peak}}| = 13.7 \text{ J kg}^{-1} \text{ K}^{-1}$ ,  $\delta T_{\text{FWHM}} = 31 \text{ K}$ ), and  $444 \text{ J kg}^{-1}$  ( $|\Delta S_M^{\text{peak}}| = 14.8 \text{ J kg}^{-1} \text{ K}^{-1}$ ,  $\delta T_{\text{FWHM}} = 30 \text{ K}$ ) were

TABLE I. Peak magnetic entropy change  $|\Delta S_M^{\text{peak}}|$ ,  $RC-1$ ,  $RC-2$ ,  $\delta T_{\text{FWHM}}$ ,  $T_{\text{hot}}$ ,  $T_{\text{cold}}$ ,  $RC-3$ ,  $\delta T^{\text{RC-3}}$ , and  $T_{\text{hot}}$  and  $T_{\text{cold}}$  related to  $RC-3$  for as-quenched  $\text{TbNi}_2$  alloy ribbons.

|  | $\mu_0\Delta H_{\text{max}} (T)$ |      |
|--|----------------------------------|------|
|  | 2 T                              | 5 T  |
| $ \Delta S_M^{\text{peak}}  (\text{J kg}^{-1} \text{ K}^{-1})$ | 8.0                              | 13.9 |
| $RC-1 (\text{J kg}^{-1})$                                      | 166                              | 441  |
| $RC-2 (\text{J kg}^{-1})$                                      | 126                              | 338  |
| $\delta T_{\text{FWHM}} (\text{K})$                            | 20                               | 32   |
| $T_{\text{hot}} (\text{K})$                                    | 47                               | 56   |
| $T_{\text{cold}} (\text{K})$                                   | 27                               | 24   |
| $RC-3$   | 85                               | 222  |
| $\delta T^{\text{RC-3}} (\text{K})$                            | 27                               | 29   |
| $T_{\text{hot}}^{\text{RC-3}} (\text{K})$                      | 50                               | 55   |
| $T_{\text{cold}}^{\text{RC-3}} (\text{K})$                     | 23                               | 26   |

estimated from the  $\Delta S_M(T)$  curves reported in Refs. 5, 9, and 10, respectively. These are similar to the value of  $441 \text{ J kg}^{-1}$  exhibited by the alloy ribbons made in this study. It should be emphasized that this  $RC-1$  value compares favorably with several other materials with a large refrigerant capacity associated with first- and second-order magnetic phase transitions operating in a similar temperature range, such as:  $\text{TbCoC}_2$  ( $T_C = 28 \text{ K}$ ;  $RC-1 = 354 \text{ J kg}^{-1}$ ),<sup>27</sup>  $\text{NdMn}_2\text{Ge}_{0.4}\text{Si}_{0.6}$  ( $T_N = 36 \text{ K}$ ;  $RC-1 = 270 \text{ J kg}^{-1}$ ),<sup>28</sup> and  $\text{Ho}_3\text{Ni}_2$  ( $T_C = 33 \text{ K}$ ;  $RC-1 = 477 \text{ J kg}^{-1}$ ).<sup>29</sup>

Regarding  $RC$  for a specific material, an important consideration is the occurrence of hysteresis losses in the operating temperature range of a potential refrigerant cycle. In our work, the field-up and field-down  $M(\mu_0 H)$  curves up to  $\mu_0 H_{\text{max}} = 2 \text{ T}$  were measured and the hysteresis losses were negligible (less than  $\sim 1 \text{ J kg}^{-1}$ ).

Single-phase  $\text{TbNi}_2$  alloy ribbons were fabricated using a one-step solidification process by means of the melt spinning technique, thus, avoiding the need for time consuming thermal annealing. The resulting structural characterization and the magnetic and magnetocaloric properties are similar to those already reported for bulk alloys. The measured value of  $RC \sim 441 \text{ J kg}^{-1}$  for  $\text{TbNi}_2$  is comparable, or even larger than those exhibited by some of the materials previously reported as promising candidates in a similar operating temperature range. This preparation and characterization of  $\text{TbNi}_2$  alloy ribbons demonstrate the potential of this fabrication technique to produce magnetic refrigerants based on Laves phases.

The authors acknowledge the financial support received from: (a) CONACYT, Mexico (Project CB-2010-01-156932); (b) Spanish MINECO (MAT2011-27573-C04-02); Basque Government (IT-347-07); and LINAN, IPICYT. Technical support from M.Sc. G. J. Labrada-Delgado is recognized. C.F.S.V. thanks CSIC, Spain (Grant JAEPRE-08-00508).

<sup>1</sup>K. A. Gschneidner, Jr. *et al.*, *Rep. Prog. Phys.* **68**, 1479 (2005).

<sup>2</sup>N. A. de Oliveira and P. J. von Ranke, *Phys. Rep.* **489**, 89 (2010).

<sup>3</sup>P. J. von Ranke *et al.*, *J. Appl. Phys.* **93**, 4055 (2003).

<sup>4</sup>L. Li, M. Kadonaga *et al.*, *Appl. Phys. Lett.* **101**, 122401 (2012).

<sup>5</sup>A. M. Tishin and Y. I. Spichkin, *The Magnetocaloric Effect and its Applications* (IOP, Bristol, 2003).

<sup>6</sup>R. Caballero-Flores *et al.*, *Appl. Phys. Lett.* **98**, 102505 (2011).

<sup>7</sup>P. Álvarez *et al.*, *Appl. Phys. Lett.* **99**, 232501 (2011).

<sup>8</sup>P. Álvarez, P. Gorria, and J. A. Blanco, *Phys. Rev. B* **84**, 024412 (2011).

<sup>9</sup>N. K. Singh *et al.*, *J. Phys. Condens. Matter.* **18**, 10775 (2006).

<sup>10</sup>E. J. R. Plaza *et al.*, *J. Appl. Phys.* **105**, 013903 (2009).

<sup>11</sup>K. A. Gschneidner, Jr. *et al.*, *Mater. Sci. Forum* **315**, 69 (1999).

<sup>12</sup>M. E. Wood and W. H. Potter, *Cryogenics* **25**, 667 (1985).

<sup>13</sup>E. Gratz *et al.*, *J. Phys. Condens. Matter* **11**, 7893 (1999).

<sup>14</sup>A. Lindbaum *et al.*, *Phys. Rev. B* **65**, 134114 (2002).

<sup>15</sup>M. Latroche *et al.*, *J. Less-Common Met.* **161**, L27 (1990).

<sup>16</sup>M. Latroche *et al.*, *Z. Phys. Chem.* **179**, 261 (1993).

<sup>17</sup>E. A. Skrabek and W. E. Wallace, *J. Appl. Phys.* **34**, 1356 (1963).

<sup>18</sup>G. P. Felcher *et al.*, *J. Appl. Phys.* **36**, 1001 (1965).

<sup>19</sup>O. Gutfleisch *et al.*, *J. Appl. Phys.* **97**, 10M305 (2005).

<sup>20</sup>A. Yan *et al.*, *J. Appl. Phys.* **99**, 08K903 (2006).

<sup>21</sup>T. Zhang, Y. Chen, and Y. Tang, *J. Phys. D: Appl. Phys.* **40**, 5778 (2007).

<sup>22</sup>B. Hernando *et al.*, *Appl. Phys. Lett.* **94**, 222502 (2009).

<sup>23</sup>J. L. Sánchez Llamazares *et al.*, *J. Appl. Phys.* **111**, 07A932 (2012).

<sup>24</sup>Z. B. Li *et al.*, *Appl. Phys. Lett.* **100**, 174102 (2012).

<sup>25</sup>J. Rodríguez-Carvajal, *Physica B* **192**, 55 (1993).

<sup>26</sup>P. Gorria *et al.*, *J. Phys. D: Appl. Phys.* **41**, 192003 (2008).

<sup>27</sup>B. Li *et al.*, *Appl. Phys. Lett.* **92**, 242508 (2008).

<sup>28</sup>J. L. Wang *et al.*, *Appl. Phys. Lett.* **98**, 232509 (2011).

<sup>29</sup>Q. Y. Dong *et al.*, *Appl. Phys. Lett.* **99**, 132504 (2011).